



**HAL**  
open science

## Enzymatic fuel cells in a microfluidic environment: Status and opportunities. A mini review

Prakash Rewatkar, Vivek Pratap Hitaishi, Elisabeth Lojou, Sanket Goel

### ► To cite this version:

Prakash Rewatkar, Vivek Pratap Hitaishi, Elisabeth Lojou, Sanket Goel. Enzymatic fuel cells in a microfluidic environment: Status and opportunities. A mini review. *Electrochemistry Communications*, 2019, 107, pp.106533. 10.1016/j.elecom.2019.106533 . hal-02375006

**HAL Id: hal-02375006**

**<https://hal.science/hal-02375006>**

Submitted on 21 Nov 2019

**HAL** is a multi-disciplinary open access archive for the deposit and dissemination of scientific research documents, whether they are published or not. The documents may come from teaching and research institutions in France or abroad, or from public or private research centers.

L'archive ouverte pluridisciplinaire **HAL**, est destinée au dépôt et à la diffusion de documents scientifiques de niveau recherche, publiés ou non, émanant des établissements d'enseignement et de recherche français ou étrangers, des laboratoires publics ou privés.



## Enzymatic fuel cells in a microfluidic environment: Status and opportunities. A mini review



Prakash Rewatkar<sup>a</sup>, Vivek Pratap Hitaishi<sup>b</sup>, Elisabeth Lojou<sup>b,\*</sup>, Sanket Goel<sup>a</sup>

<sup>a</sup> MEMS and Microfluidics Lab, Department of Electrical and Electronics Engineering, Birla Institute of Technology and Science (BITS) Pilani, Hyderabad Campus, 500078 Hyderabad, India

<sup>b</sup> Aix Marseille Univ, CNRS, BIP, Bioénergétique et Ingénierie des Protéines, 31 chemin Aiguier, 13402 Marseille, France

### ARTICLE INFO

#### Keywords:

Enzyme  
Biofuel cell  
Microfluidic  
Membraneless  
Microfabrication

### ABSTRACT

Miniaturized Enzymatic Fuel Cells (EFCs) have attracted great attention due to the possibility of integrating them with various low-powered microelectronic devices. In a flow-through system, harnessing the co-laminar property of microfluidics, membraneless microfluidic EFCs (M-MEFC) can be designed, enhancing the ease of use of bio-devices and offering opportunities for new concepts. This brief review encompasses the development, current challenges and future pathways in the field of M-MEFCs, focusing in particular on some fabrication aspects and related device performance.

### 1. Introduction

Enzymatic fuel cells (EFCs) have emerged as an eco-friendly energy-producing technology based on the capacity of naturally available redox enzymes to transform a wide diversity of fuels and oxidants with high specificity and high efficiency [1–4]. Since the proof of concept of a glucose/O<sub>2</sub> EFC, increased power outputs over longer periods have been reported, mainly thanks to improved knowledge of the molecular basis for high direct electron transfer rates between enzymes and high surface/volume nanomaterials [5–7]. New enzymes have been identified, especially from extremophilic microorganisms, improving long-term stability, but also allowing non-glucose-based EFCs to be developed [8]. However, many challenges persist, hindering their pathway towards cost-effectiveness, miniaturization and automation while maintaining the high performance necessary for commercial applications [9,10]. Harnessing the unique features of micro- and nanoscale technology enables the EFC to consume less power, to achieve precise control and easy manipulation of fluids, as well as providing a quick response to reactants and a high surface to volume ratio (SVR), making them suitable for integration with various systems [11,12].

Microfluidics is concerned with the technology and systems used for processing and manipulating very small volumes of fluids, from microliters (μl, 10<sup>-6</sup>) to femtoliters (fl, 10<sup>-15</sup>). These devices offer many advantages over more conventional devices, including (i) increase in rates of reaction, (ii) decrease in power consumption, (iii) integration with other lab-on-chip devices, (iv) ease and control of disposing of

devices and fluids, (v) reduced reagent cost, (vi) higher surface to volume ratio, (vii) low Reynolds number, and (viii) minimized size of the chip [13]. If applied to EFCs, the co-laminar regime permits the development of membraneless microfluidic EFCs (M-MEFC) [14]. M-MEFCs are currently becoming more commercially viable, and can be used as a source of electric power for portable and implantable devices such as neurophysiological monitors, insulin pumps, brain simulators, continuous glucose monitors and glucose-sensing contact devices [15], as self-powered glucose biosensors [16], or wireless networks [17,18].

The aim of this mini review is to report the main advances in M-MEFCs over the past five years. It briefly discusses the fundamentals of microfluidics technology, in terms of scaling and fluid flow characteristics, and how it may be utilized to develop M-MEFCs, focusing on cell component dimensions, materials, easy and environmentally friendly fabrication, and overall polarization performance metrics such as open circuit potential (OCP), current density (CD), and power density (PD). Finally, the review describes some potential applications of M-MEFCs and looks at future opportunities.

### 2. Basic fundamentals of microfluidics

#### 2.1. Summary of principle

Microfluidics is a multidisciplinary technology involving the manufacture of devices and manipulation of fluids in a micro- and nano-environment, exploiting various characteristics such as reliability,

\* Corresponding author.

E-mail address: [lojou@imm.cnrs.fr](mailto:lojou@imm.cnrs.fr) (E. Lojou).

<https://doi.org/10.1016/j.elecom.2019.106533>

Received 28 June 2019; Received in revised form 26 August 2019; Accepted 26 August 2019

Available online 27 August 2019

1388-2481/ © 2019 The Authors. Published by Elsevier B.V. This is an open access article under the CC BY-NC-ND license (<http://creativecommons.org/licenses/by-nc-nd/4.0/>).

robustness, automation and long-term stability. This rapidly emerging technology offers completely new opportunities and breakthroughs in research fields including fluid handling, biomedicine, proteomics, genetics, optic, and energy [19].

A few reviews on microfluidic fuel cells, including some fundamentals of microfluidics, have been reported previously [14,20,21]. Briefly, when manipulating fluids at the sub-millimeter length scale in a microchannel, the surface and interfacial tension (surface-to-fluid and fluid-to-fluid), capillary forces and laminar flow are crucial concepts [22]. The Reynolds number ( $Re$ ) related to fluid flow, which equates the inertial force to the viscous force, is smaller than in other flow systems. A typically low  $Re$  number ( $Re < \sim 2000$ ) allows laminar fluid flow rather than turbulence ( $Re > \sim 2000$ ) [23]. These concepts allow the development of miniaturized microfluidic devices well suited for bio-sensing, DNA and PCR analysis [24], glucose monitoring [25], defense applications, etc. In the last ten years, extensive work has been carried out towards the development of such devices, including mathematical modeling, computational simulation, fabrication, characterization, and testing. A lot of miniature microfluidic devices are now commercially viable having been endorsed after passing rigorous clinical tests [26]. This has led to a huge motivation to develop new microfluidic EFCs (MEFCs) and take them to a commercial scale.

## 2.2. EFCs in a microfluidic environment

Small dimensions provide an opportunity to enhance mass transfer rates, reaction rates and cell voltages at low volume. The miniaturization of EFCs leverages further advantages at the microscale: faster response times, reagent volume reduction, automated fluid delivery, lower operational costs and a high SVR, which scales as the inverse of the characteristic length over the size of the EFCs. Further, microfluidic EFCs are compatible with some simple microfabrication technologies, such as conventional soft lithography, rapid prototyping xurography and paper-based techniques. However, when reducing the total cell volume from a macroscale to a microscale, a major improvement is required to successfully develop MEFCs, especially in the areas of device fabrication, electrode architecture and dedicated electrochemistry.

In classical Pt-based fuel cells, a physical barrier (a membrane separator), separating anolyte and catholyte solutions where fuel and oxidant exchange ions, enables effective mass transport [27]. Although the specificity of redox enzymes a priori makes it possible to avoid any membrane separator, cross-reactions are expected to lower the power output and may induce severe enzyme inhibition by generation of reactive oxygen species, for example. In the particular case of the recently developed  $H_2/O_2$  EFCs, there is a requirement for a membrane impermeable to gases in order to avoid explosion hazards [5]. At the same time, the membrane separator induces high internal resistance as well as being potentially toxic towards redox enzymes, leading to a further decrease in the power conversion potential of EFCs [19,28]. Furthermore, the separator membrane makes biofuel cells bulky and costly, and shortens the cell life. Hence, there is a great incentive to work on the development of membraneless MEBFCs, while taking into account associated parameters such as cell design and size, electrode architecture, fluid delivery, manipulation systems, etc.

## 2.3. Principle to develop M-MEFCs

Fundamental research has been directed at the optimization of flow characteristics in a micro-environment, where fluids can be precisely guided and manipulated in small microfluidic channels in the microliters to femtoliters range [13]. With these advanced techniques, portable, reliable research platforms fully integrating microfluidic membraneless EFCs (M-MEFC) could potentially be developed [20].

By establishing a co-laminar flow, M-MEFCs benefit from the fluid–fluid streaming interface, slowing down the mixing of anolyte and catholyte, thus eliminating the need for a physical membrane and the

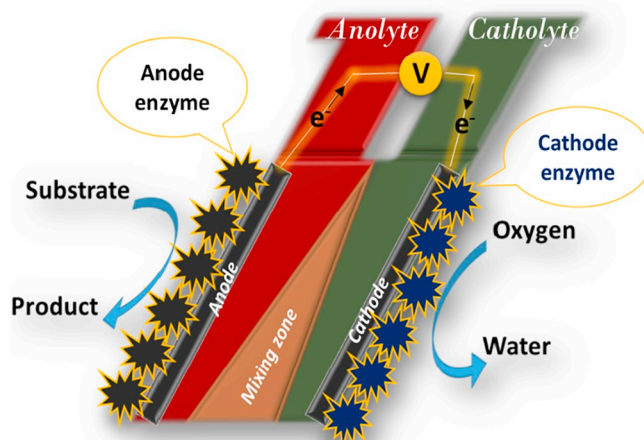


Fig. 1. Schematic representation of M-MEFCs.

associated fabrication costs associated with conventional EFCs (Fig. 1). As the dimensions of microfluidic channels are reduced in size (1–1000  $\mu\text{m}$ ), viscous forces dominate inertial forces due to the fluid flow. However, the co-laminar fluid flow is established due to a low Reynolds number ( $Re < 2000$ ) when the density and viscosities of two different fluids are ultimately analogous in the microfluidic channel. This parallel fluid–fluid flow develops a functional interface which serves as a virtual layer to differentiate the two fluids in the same microchannel [29]. Even though the ionic exchange happens across the co-laminar interface along the length of the microchannel, the fuel and oxidant flow as parallel streams. Diffusion is the primary phenomenon enabling mixing of the two streams. Mixing is limited to a narrow interfacial zone, whose thickness can be controlled by the microchannel dimensions and flow rates. A major interest in using M-MEFCs is the possibility to use different electrolytes on the anode and cathode sides, allowing the optimum pH for each enzyme to be used. Furthermore, in such scenario, the drawback of slow diffusion of protons could be overcome by optimizing the distance between the two electrodes.

## 3. Enzymes and related substrates used in M-MEFCs

Key components of EFCs are anodic and cathodic enzymes. Glucose/ $O_2$  devices remain the most largely studied and developed M-MEFCs, so glucose oxidase (GOx), or glucose dehydrogenase (GDH), and laccase (LAC) or bilirubin oxidase (BOD) are the most widely used enzymes for the anodic and cathodic side, respectively. Two other types of M-MEFC have been reported, based on lactate oxidase [30] or alcohol dehydrogenase at the anode [31], for lactate oxidation and alcohol oxidation, respectively. There is a growing interest in developing  $H_2/O_2$  M-MEFCs based on hydrogen oxidation by hydrogenases at the anode [10], due to their ability to deliver very high PD [32]. In this case, it is all the more important to separate the fuel and the oxidant, not only to avoid an explosion hazard but also to prevent hydrogenase inactivation by  $O_2$ . Although microfluidic  $H_2/O_2$  fuel cells have been described [33],  $H_2/O_2$  M-MEFCs have not yet been reported, to the best of our knowledge.

For the immobilization of these redox enzymes, a variety of procedures are available on different electrode materials with (mediated electron transfer, MET) or without (direct electron transfer, DET) the use of additional reagents to mediate the biocatalysis. Relevant references can be found in recent reviews [6,7,34]. In DET mode, the electrochemical reaction occurs between the active site of enzymes, or a cofactor acting as an electron relay, and the electrode surface. This reaction is advantageous because it does not require any additional redox component and operates at the redox potential of the associated enzyme, hence with a low overpotential. In the case of an unfavorable enzyme orientation, or inaccessible electron relay available close to the

**Table 1**  
Fabrication, components and performance of M-MEFCs.

Fabrication technique	Fuel	Oxidant	Anode material	Cathode material	M-MEFC performance			Ref
					OCP mV	Max CD	Max PD	
Soft lithography Flow rate: 1000 $\mu\text{h}^{-1}$	100 mM glucose	O <sub>2</sub>	<i>Aspergillus niger</i> GOx covalently bound to SWCNT; MET with FEMOL	<i>Bacillus subtilis</i> LAC covalently bound to SWCNT; MET with ABTS	440	7 $\mu\text{A}\cdot\text{cm}^{-2}$	1.65 $\mu\text{W}\cdot\text{cm}^{-2}$	[40]
Soft lithography	100 mM glucose	O <sub>2</sub>	GOx on carbon paste; MET with ferrocene	BOD on carbon paste DET mode	180	–	0.98 $\mu\text{W}\cdot\text{cm}^{-2}$	[39]
Soft lithography Flow rate: 0.35 ml·min <sup>-1</sup>	27 mM glucose	O <sub>2</sub>	<i>A. niger</i> GOx on porous gold; MET with ferrocene; DET mode	<i>Rhus vernicifera</i> LAC covalently bound to porous gold; DET mode	340	10 $\mu\text{A}\cdot\text{cm}^{-2}$	1.6 $\mu\text{W}\cdot\text{cm}^{-2}$	[42]
Soft lithography Flow rate: 0.35 ml·min <sup>-1</sup>	27 mM glucose	O <sub>2</sub>	<i>A. niger</i> GOx on porous gold; MET with ferrocene; DET mode	<i>Rhus vernicifera</i> LAC on porous gold; DET mode	350	–	2.75 $\mu\text{W}\cdot\text{cm}^{-2}$	[43]
Xurography Flow rate: 70 $\mu\text{l}\cdot\text{min}^{-1}$	100 mM glucose	O <sub>2</sub>	<i>A. niger</i> GOx in a redox polymer; MET mode	<i>Trametes versicolor</i> LAC on MWCNT; DET mode	540	290 $\mu\text{A}\cdot\text{cm}^{-2}$	64 $\mu\text{W}\cdot\text{cm}^{-2}$	[45]
Xurography Flow rate: 150 $\mu\text{l}\cdot\text{min}^{-1}$ Vertical stacking	10 mM glucose	O <sub>2</sub>	<i>A. niger</i> GOx in solution; MET with Fe(CN) <sub>6</sub> <sup>3-</sup>	<i>Trametes versicolor</i> LAC in solution; MET with ABTS	390	85 $\mu\text{A}$	12 $\mu\text{W}$	[17]
Xurography Flow rate: 100 $\mu\text{l}\cdot\text{min}^{-1}$ Multi-level channel distribution	100 mM glucose	O <sub>2</sub>	<i>A. niger</i> GOx in solution; MET with Fe(CN) <sub>6</sub> <sup>3-</sup>	<i>Trametes versicolor</i> LAC in solution; MET with ABTS	384	77.5 $\mu\text{A}$	13.37 $\mu\text{W}$	[46]
Xurography Flow rate: 500 $\mu\text{l}\cdot\text{min}^{-1}$ Cantilevered bioelectrode	Alcohol	O <sub>2</sub>	Alcohol dehydrogenase; MET mode with PMG	LAC; MET mode with ABTS	630	2.9 mA·cm <sup>-3</sup>	13.8 $\mu\text{W}\cdot\text{cm}^{-2}$ 1.25 mW·cm <sup>-3</sup>	[31]
Paper-based	100 mM glucose	O <sub>2</sub>	GDH; MET with PMG on BP	BOD; DET	620	1 mA	180 $\mu\text{W}/\text{mg}$ GDH (3 series)	[47]
Paper-based	100 mM glucose	O <sub>2</sub>	<i>A. niger</i> GOx in a redox polymer; MET mode	<i>T. versicolor</i> LAC on MWCNT; DET mode	600 (Y-shaped)	320 $\mu\text{A}\cdot\text{cm}^{-2}$ (Y-shaped)	45 $\mu\text{W}\cdot\text{cm}^{-2}$ (Y-shaped)	[49]
Paper-based Volume of 35 $\mu\text{l}$	2.5 to 100 mM glucose	O <sub>2</sub>	<i>Aspergillus</i> sp. GDH in a redox polymer; MET mode	<i>Myrothecium</i> BOD in a redox polymer; MET mode	555 (I-shaped) 650 (I-shaped)	225 $\mu\text{A}\cdot\text{cm}^{-2}$ (I-shaped) 275 $\mu\text{A}\cdot\text{cm}^{-2}$ (I-shaped)	24 $\mu\text{W}\cdot\text{cm}^{-2}$ (I-shaped) 97 $\mu\text{W}\cdot\text{cm}^{-2}$ (I-shaped)	[50]
Paper-based	40 mM glucose	O <sub>2</sub>	<i>A. niger</i> GOx covalently bound to BP; MET mode with benzoquinone	<i>T. versicolor</i> LAC covalently bound to BP; MET with ABTS	570	600 $\mu\text{A}\cdot\text{cm}^{-2}$	100 $\mu\text{W}\cdot\text{cm}^{-2}$	[48]
Paper-based Screen-printed circular type	100 mM glucose	O <sub>2</sub>	GOx on porous carbon; MET mode	<i>Myrothecium</i> BOD on porous carbon; DET mode	2.65 mV	305 $\mu\text{A}$ (at 0 V)	70 $\mu\text{W}\cdot\text{cm}^{-2}$ (5 series)	[52]
Paper-based Origami array-type	100 mM glucose	O <sub>2</sub>	GOx on porous carbon; MET mode	<i>Myrothecium</i> BOD in MgO-templated porous carbon; DET mode	950	480 $\mu\text{A}\cdot\text{cm}^{-2}$	180 $\mu\text{W}\cdot\text{cm}^{-2}$ (2 series)	[53]
Paper-based array-type	100 mM glucose	O <sub>2</sub>	GOx on porous carbon; MET mode	<i>Myrothecium</i> BOD in MgO-templated porous carbon; DET mode	2.30 mV	1040 $\mu\text{A}$	60 $\mu\text{W}\cdot\text{cm}^{-2}$ (4 series/4 parallel)	[54]
Paper-based capillary induced flow	5 mM glucose	O <sub>2</sub>	<i>Aspergillus</i> sp. GDH in a redox polymer on MWCNT; MET mode	<i>Myrothecium</i> BOD on MWCNT with Nafion; DET mode	710	70 $\mu\text{A}\cdot\text{cm}^{-2}$	37.5 $\mu\text{W}\cdot\text{cm}^{-2}$	[51]

FEMOL: ferrocene methanol; ABTS: 2,2'-azinobis(3-ethylbenzothiazoline-6 sulfonate); PMG: polymethylene green; BP: bucky paper.

surface of the enzymes, the MET mode allows interfacial electron transfer, but at the same time increases the overall cost and complicates the immobilization strategy [35]. MET may also induce overpotentials which decrease the overall power output. Note that some M-MEBFCs have been reported based on a DET process for glucose oxidation by GOx – it should be borne in mind that DET is possibly slow and potentially unexpected due to the isolation of the active site of GOx in the protein moiety [36].

As noted above, O<sub>2</sub> is mainly used as the oxidant in M-MEBFCs. Low oxygen solubility, and the impact of O<sub>2</sub> or oxygen reaction species on many enzymes require technical strategies to be developed. Decreasing

the distance between the electrodes will decrease the internal cell resistance [37], but will increase the mixing zones, highlighting that cell geometry is a critical factor in M-MEBFCs.

#### 4. Fabrication methods for M-MEFCs

There are several well-developed methods for fabricating microfluidic devices. Details of the M-MEFCs reported in the last five years in terms of OCP and PD are reported in Table 1, together with information on the device fabrication techniques, enzymes and catalytic mechanisms involved.

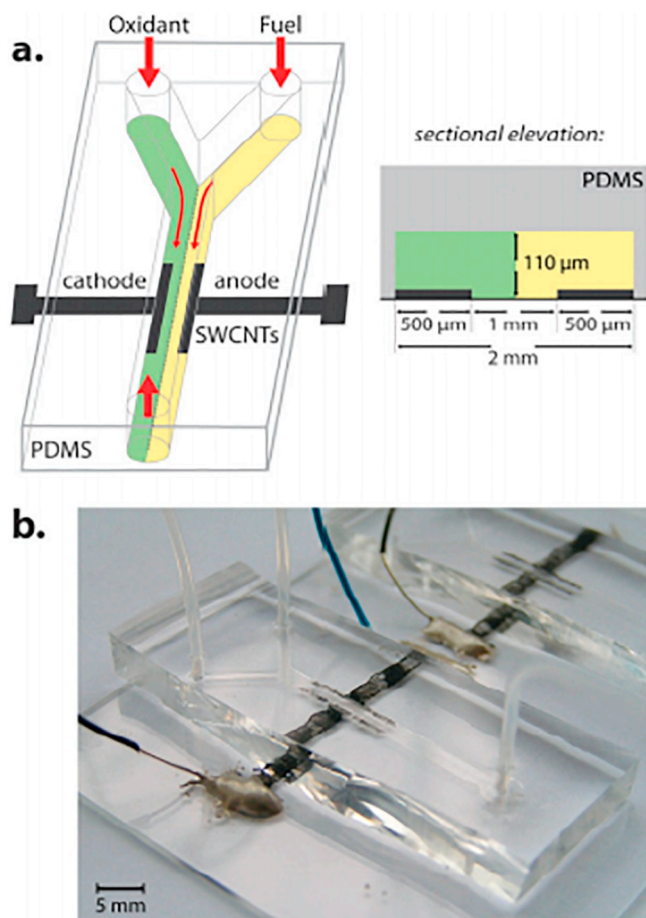


Fig. 2. (a) Schematic view of Y-shaped M-MEFC embedding two electrodes showing the co-laminar fluid flow inside the microchannel and (b) fully assembled photograph of the Y-shaped M-MEFC. (Replicated from [40] with permission from the Royal Society of Chemistry.)

#### 4.1. Soft lithography

Soft lithography provides a set of smart tools for the fabrication and manufacture of prototypes by molding and embossing an elastomeric liquid organic polymer such as poly(dimethylsiloxane) (PDMS). PDMS has attracted attention in the microfluidic field as it is simple and easy to make, cost-effective, biocompatible, and optically clear and flexible [38].

Soft lithography-based techniques have been used to design M-MEFCs with different geometries: T-shaped, Y-shaped or I-shaped (Fig. 2). Enzymes were either adsorbed on carbon paste [39] or covalently attached onto single-walled carbon nanotubes (SWCNT) [40]. Covalent binding of enzymes is expected to decrease the amount of biomolecule required, and increase cell stability. However, depending on the way the covalent attachment is achieved, a decrease in enzymatic activity may arise [41]. Great improvements in the performance of M-MEFCs were obtained using porous electrodes with an optimal enzyme immobilization process and improvement in the microfluidic flow. As an illustration, H. du Toit et al. [42] reported a miniature M-MEFC which generated continuous power for up to one month. Enhanced performance was achieved through a multielectrode design with series and parallel configurations [43]. The power outputs in these devices are less than  $5 \mu\text{W}\cdot\text{cm}^{-2}$ , one hundred times lower than the PD of current EFCs, but this is sufficient to run low-powered medical or sensor devices [44].

#### 4.2. Xurography

Xurography-based microfabrication techniques are widely used to make microfluidic devices, including M-MEFCs. Xurography involves using a simple cutting plotter on various flexible polymer films to create microstructures down to  $\sim 20 \mu\text{m}$ . The main features of this technique are the short fabrication time and that fact that it does not require any photolithographic processes, harsh chemicals, or clean room facilities.

González-Guerrero et al. [45] introduced xurography techniques to make M-MEFCs in 2013. The fabrication of microchannels was accomplished using a cutter and plotter, leading to the fabrication of a complete layer-by-layer M-MEBFC enclosed in poly(methylmethacrylate) material (Fig. 3). GOx embedded in redox hydrogel and LAC adsorbed on multi-walled carbon nanotubes (MWCNT) have been drop-cast on pyrolyzed photoresist films. The PD of such an M-MEFC is determined as a function of the flow rate. Subsequently, D. Desmaële et al. [17] described an M-MEFC using xurography techniques for wireless data transmission. Thin T-shaped flexible microchannels were fabricated using polymer and flexible gold electrode film via sputtering techniques. GOx and LAC were not wired to the electrodes but present in the anolyte and cathodic solutions, respectively. Low stability of the PD was noted, attributed to the formation of a depletion layer in the stack. L. Renaud et al. [46] extended this 2D T-shaped M-MEFC using multi-level methodology. A new geometry was further designed with cantilevered porous electrodes in which alcohol dehydrogenases and LAC were immobilized [30].

#### 4.3. Paper-based devices

Porous filter papers are convenient supports for cost-effective, biocompatible and disposable microfluidic devices for analytical measurement, due to their self-pumping, capillary flow behavior and high SVR. Such paper-based platforms have also been used to fabricate M-MEFCs by producing a hydrophobic barrier on the filter paper using wax printer technology and normal wax crayons to guide the electrolyte and achieve the proper micro-flow.

Early work by Atanassov's group [47] demonstrated that paper-based M-MEFCs were able to resolve the mass transfer limitation of classical EFCs. The anode was composed of bucky paper (BP) on which a redox polymer with embedded GDH was immobilized, while BOD was the biocatalyst at the cathode. A 3-cell stack in series powered a digital clock for 9 h. Very recently, Rewatkar et al. [48] presented a cost-effective paper-based M-MEFC with greatly enhanced performance ( $100 \mu\text{W}\cdot\text{cm}^{-2}$ ) (Fig. 4). The open circuit potential remained stable for 50 h. However, high concentrations of redox mediators were used, which could impact the overall process. González-Guerrero et al. [49] introduced a Y-shaped co-laminar fluid flow M-MEFC, using carbon papers as bioelectrodes. Nafion was added to the biocathodic ink to ensure proton conduction, and to prevent oxygen diffusion at the anode side. A one-stream fuel cell (I-shaped) was also designed which had a smaller PD, but demonstrated the capability of this very simple configuration. Later, the same group [50] developed a paper-based platform for the detection of glucose in practical conditions, i.e. a volume equivalent to a drop of blood, and a glucose concentration compatible with physiological concentrations.

One issue of paper-based M-MEFCs is low  $\text{O}_2$  availability, which induces cathodic limitations. In classical EFCs, this issue is overcome by enlarging the cathode surface compared to the anode, a solution that cannot be applied to M-MEFCs. Del Torno-de Román et al. proposed instead to tune the capillary flow upon the cathode [51]. One other challenge is to reach the voltage level required to power electronic devices. New M-MEFCs geometries have therefore been developed [52,53]. Shitanda et al. showed a circular-type paper-based M-MEFC combining five individual cells in series that produces an OCP of 2.65 V and a power of  $350 \mu\text{W}$  [52]. A stack of 4-series/4-parallel paper-based cells reached a PD of  $970 \mu\text{W}$  at 1.4 V [54], highlighting a net

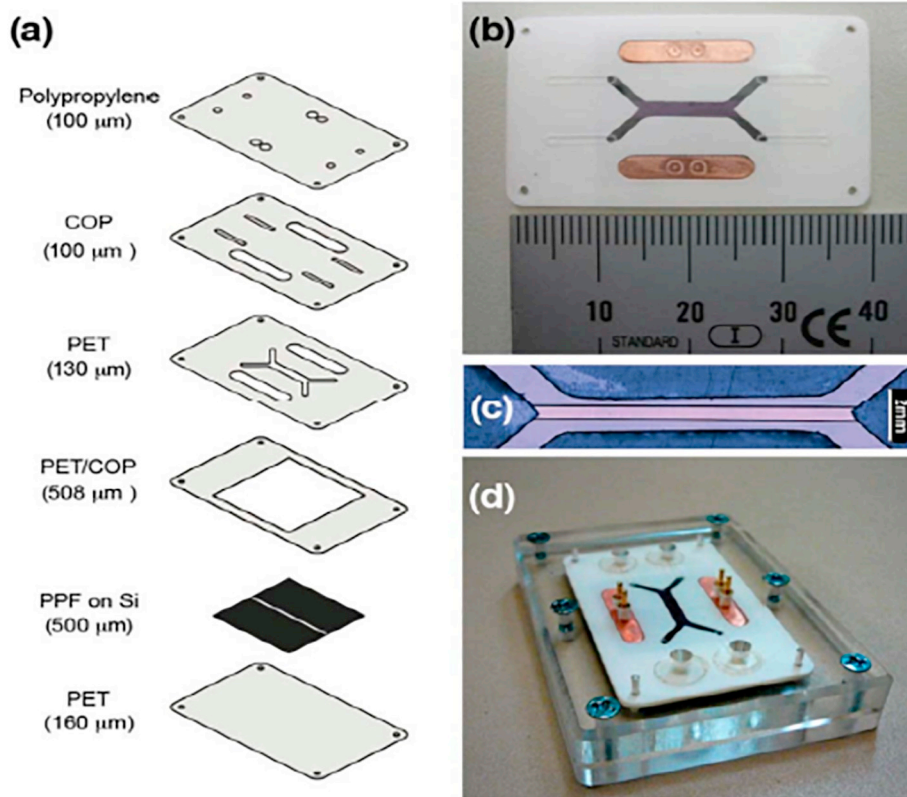


Fig. 3. (a) Schematic view of the complete stepwise fabrication process of two inlets and two outlets M-MEFC, (b) fully integrated design, (c) cross-sectional view of microchannel and electrode, and (d) actual picture of the final device. (Replicated from [45] with permission from the Royal Society of Chemistry.)

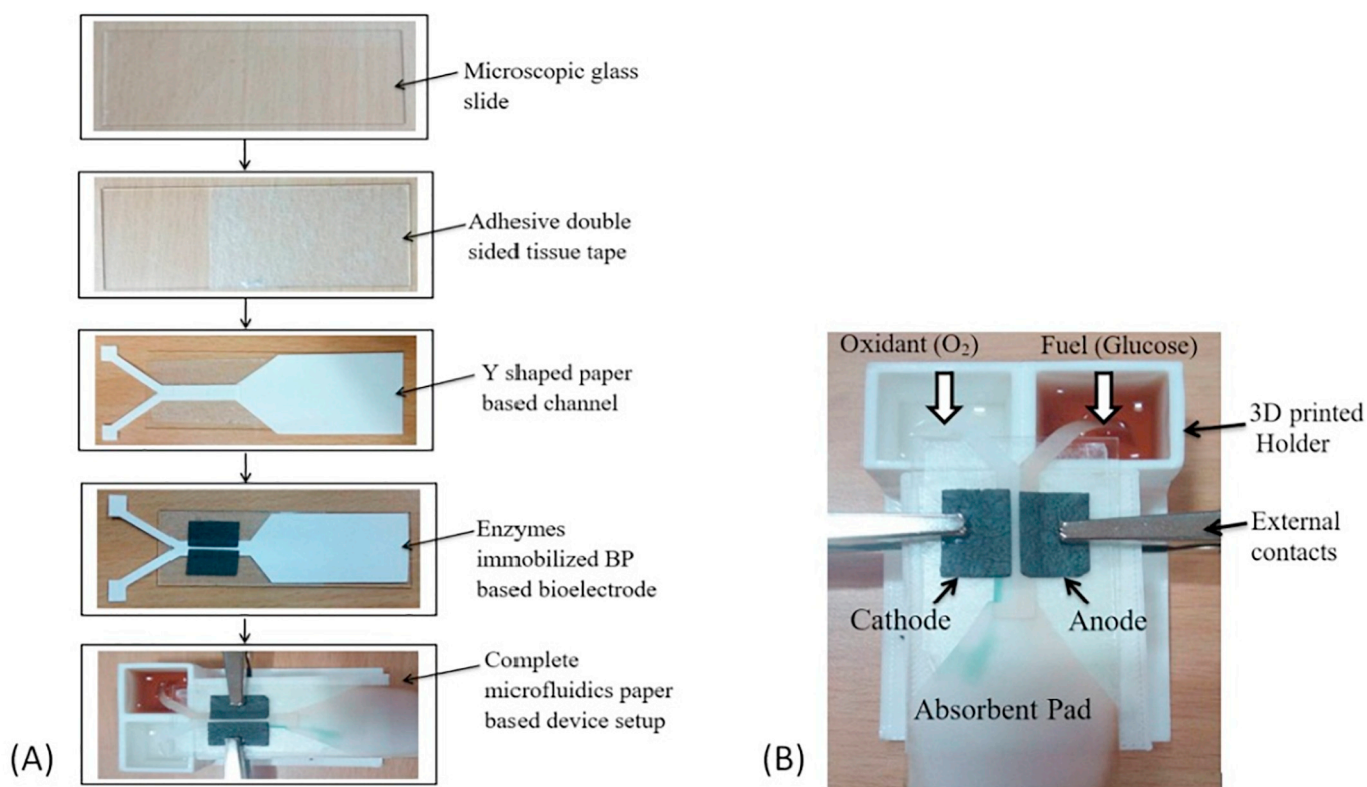


Fig. 4. (A) A schematic view of the step by step fabrication of Y-shaped paper-based M-MEFC and (B) picture of fully integrated Y-shaped paper-based M-MEFC. (Replicated from [48] with permission from IEEE Transactions on NanoBioscience.)

improvement in M-MEFC performance.

Comparing the various methods, one major difference comes from the passive pumping required for soft lithography and xurography, while in paper-based devices self-pumping leads to the fluid flow. Therefore, in paper-based devices the flow rate depends only on the paper type, meaning that for a given platform the flow-rate is fixed, whereas in other two techniques the flow rate can be adjusted according to the experimental requirements.

## 5. Conclusion and future pathway

This mini review highlights the improved performances of M-MEFCs thanks to bioelectrode integration in co-laminar microfluidic systems. Application areas include energy generation, especially in remote places; energy conversion and storage via supercapacitors; and in vivo operation, taking advantage of the availability of fuels (glucose, lactate) in bodily physiological fluids such as urine, saliva, and tears, to power sensing or micro-recording devices. Extension of M-MEFC to H<sub>2</sub>/O<sub>2</sub> EBFCs is a completely new concept that may allow the use of such high performing devices in a self-powered and disposable manner.

If these types of devices are to be adopted by the scientific community there is a strong need for further improvement of existing fabrication technologies, to produce higher power densities and self-sustainable energy production, together with economical fabrication and maintenance cost. As summarized here, the power densities delivered by most reported M-MEFCs are lower than those obtained using conventional EFCs. Mass transfer limitations must be improved, for example by tuning the geometry of the cell, in particular the length of the microchannel. The architecture of the microchannel must also be improved to decrease the mixing zone and avoid substrate depletion zones. Modeling and simulation of flow kinetics should help in device optimization. Another source of low power output is the poor electron transfer between enzymes and electrodes. Many questions remain regarding the efficiency of the wiring of enzymes on electrodes: what are the conformations of immobilized enzymes and their evolution with applied potential, what is the effect of enzyme density, what is the effect of local pH variation, etc. This fundamental knowledge is required to optimize the loading, stability, and electroactivity of bioelectrodes to design more efficient M-MEFCs. In addition, the discovery of new enzymes with higher stability against changes in salinity, pH, temperature, and the presence of inhibitors, as well as developments in enzyme engineering will open the way for new applications of M-MEBFCs. Multidisciplinary approaches as well as new methods coupled with electrochemistry are urgently required for the future development of M-MEBFCs.

## Acknowledgements

This work was financially supported by Agence Nationale de la Recherche (ENZYMO-ANR-16-CE05-0024), and by Aix-Marseille University for funding V.P. Hitaishi.

## References

- [1] D. Kashyap, P.S. Venkateswaran, P.K. Dwivedi, Y.H. Kim, G.M. Kim, A. Sharma, S. Goel, *Int. J. Nanoparticles* 8 (2015) 61–81.
- [2] M. Gamella, A. Koushanpour, E. Katz, *Bioelectrochem* 119 (2018) 33–42.
- [3] J. Kim, A.S. Campbell, B.E.F. de Ávila, J. Wang, *Nat. Biotechnol.* 37 (2019) 389–406.
- [4] X. Xiao, H. Xia, R. Wu, L. Bai, L. Yan, E. Magner, S. Cosnier, E. Lojou, Z. Zhu, A. Liu, *Chem. Rev.* (2019), <https://doi.org/10.1021/acs.chemrev.9b00115>.
- [5] I. Mazurenko, K. Monsalve, J. Rouhana, P. Parent, C. Laffon, A. Le Goff, S. Szunerits, R. Boukherroub, M.T. Giudici-Ortoniconi, N. Mano, E. Lojou, *ACS Appl. Mater. Interfaces* 8 (2016) 23074–23085.
- [6] V.P. Hitaishi, I. Mazurenko, M. Harb, R. Clément, M. Taris, S. Castano, D. Duché, S. Lecomte, M. Ilbert, A. de Poulpique, E. Lojou, *ACS Catal.* 8 (2018) 12004–12014.
- [7] I. Mazurenko, A. de Poulpique, E. Lojou, *Curr. Op. Electrochem.* 5 (2017) 74–84.
- [8] I. Mazurenko, X. Wang, A. de Poulpique, E. Lojou, *Sust. Energ. Fuels* 1 (2017) 1475–1501.
- [9] J. Yang, S. Ghobadian, P.J. Goodrich, R. Montazami, N. Hashemi, *Phys. Chem. Chem. Phys.* 15 (2013) 14147–14161.
- [10] A. Zebda, J.P. Alcaraz, P. Vadgama, S. Shleev, S.D. Minteer, F. Boucher, P. Cinquin, D.K. Martin, *Bioelectrochem* 124 (2018) 57–72.
- [11] M.H. Osman, A.A. Shah, F.C. Walsh, *Biosens. Bioelectron.* 26 (2011) 3087–3102.
- [12] S.D. Minteer, B.Y. Liaw, M.J. Cooney, *Curr. Op. Biotech.* 18 (2007) 228–234.
- [13] M. Safdar, J. Jänis, S. Sánchez, *Lab Chip* 16 (2016) 2754–2758.
- [14] E. Kjeang, N. Djilali, D. Sinton, *J. Power Sources* 186 (2009) 353–369.
- [15] P. Rewatkar, M. Bandapati, S. Goel, *IEEE Sensors J.* 18 (2018) 5395–5401.
- [16] G. Slaughter, T. Kulkarni, *Energies* 12 (2019) 825.
- [17] D. Desmaële, L. Renaud, S. Tingry, *Sensors Actuators B Chem.* 220 (2015) 583–589.
- [18] K. Monsalve, I. Mazurenko, N. Lalaoui, A. Le Goff, M. Holzinger, P. Infossi, S. Nitsche, J.Y. Lojou, M.T. Giudici-Ortoniconi, S. Cosnier, E. Lojou, *Electrochem. Commun.* 60 (2015) 216–220.
- [19] D. Di Carlo, *Lab Chip* 9 (2009) 3038–3046.
- [20] Y. Yang, T. Liu, K. Tao, H. Chang, *Ind. Eng. Chem. Res.* 57 (2018) 2746–2758.
- [21] J.W. Lee, E. Kjeang, *Biomicrofluidics* 4 (2010) 041301.
- [22] M.A. Goulet, E. Kjeang, *J. Power Sources* 260 (2014) 186–196.
- [23] P.J.A. Kenis, R.F. Ismagilov, G.M. Whitesides, *Sci* 285 (1999) 83–85.
- [24] D. Erickson, D.Q. Li, *Anal. Chim. Acta* 507 (2004) 11–26.
- [25] C.J. Huang, Y.H. Chen, C.H. Wang, T.C. Chou, G.B. Lee, *Sensors Actuators B Chem.* 122 (2007) 461–468.
- [26] V. Faustino, S.O. Catarino, R. Lima, G. Minas, *J. Biomech.* 49 (2016) 2280–2292.
- [27] Z. Ghassemi, G. Slaughter, *Membranes* 7 (2017) 3.
- [28] H.Z. Wang, S.J. Gu, D.Y.C. Leung, H. Xu, M.K.H. Leung, L. Zhang, J. Xuan, *Electrochim. Acta* 135 (2014) 467–477.
- [29] S.A. Mousavi Shaegh, N.-T. Nguyen, S.H. Chan, *Int. J. Hydrog. Energy* 36 (2011) 5675–5694.
- [30] R.A. Escalona-Villalpando, R.C. Reid, R.D. Milton, L.G. Arriaga, S.D. Minteer, J. Ledesma-García, *J. Power Sources* 342 (2017) 546–552.
- [31] D. Desmaële, T.T. Nguyen-Boisse, L. Renaud, S. Tingry, *Microelectron. Eng.* 165 (2016) 23–26.
- [32] I. Mazurenko, K. Monsalve, P. Infossi, M.T. Giudici-Ortoniconi, F. Topin, N. Mano, E. Lojou, *Energy Environ. Sci.* 10 (2017) 1966–1982.
- [33] J.P. Esquivel, J.R. Buser, C.W. Lim, C. Domínguez, S. Rojas, P. Yager, N. Sabaté, *J. Power Sources* 342 (2017) 442–451.
- [34] N. Mano, A. de Poulpique, *Chem. Rev.* 118 (2018) 2392–2468.
- [35] S.A. Neto, J.C. Forti, A.R. De Andrade, *Electrocatalysis* 1 (2010) 87–94.
- [36] P.N. Bartlett, F.A. Al-Lolage, *J. Electroanal. Chem.* 819 (2018) 26–37.
- [37] Y. Yang, D. Ye, J. Li, X. Zhu, Q. Liao, B. Zhang, *J. Power Sources* 324 (2016) 113–125.
- [38] P. Rewatkar, S. Balpande, J. Kalambe, *Indian J. Sci. Technol.* 11 (2018), <https://doi.org/10.17485/ijst/2018/v11i36/96827>.
- [39] Y. Fujimigari, Y. Fukushi, Y. Nishioka, *J. Photopolym. Sci. Technol.* 28 (2015) 357–361.
- [40] T. Beneyton, I.P.M. Wijaya, C. Ben Salem, A.D. Griffiths, V. Taly, *Chem. Commun.* 49 (2013) 1094–1096.
- [41] C. Gutierrez-Sanchez, A. Ciaccafava, P.Y. Blanchard, K. Monsalve, M.T. Giudici-Ortoniconi, S. Lecomte, E. Lojou, *ACS Catal.* 6 (2016) 5482–5492.
- [42] H. du Toit, M. Di Lorenzo, *Biosens. Bioelectron.* 69 (2015) 199–205.
- [43] H. du Toit, R. Rashidi, D.W. Ferdani, M.B. Delgado-Charro, C.M. Sangan, M. Di Lorenzo, *Biosens. Bioelectron.* 78 (2016) 411–417.
- [44] S. Cosnier, A. Le Goff, M. Holzinger, *Electrochem. Commun.* 38 (2014) 19–23.
- [45] M.J. González-Guerrero, J.P. Esquivel, D. Sánchez-Molas, P. Godignon, F.X. Muñoz, F.J. del Campo, F. Giroud, S.D. Minteer, N. Sabaté, *Lab Chip* 13 (2013) 2972–2979.
- [46] L. Renaud, D. Selloum, S. Tingry, *Microfluid. Nanofluid.* 18 (2015) 1407–1416.
- [47] C.W. Narváez Villarrubia, C. Lau, G.P.M.K. Ciniato, S.O. Garcia, S.S. Sibbett, D.N. Petsev, S. Babanova, G. Gupta, P. Atanassov, *Electrochem. Commun.* 45 (2014) 44–47.
- [48] P. Rewatkar, S. Goel, *IEEE Trans. NanoBiosci.* 17 (2018) 374–379.
- [49] M.J. González-Guerrero, F.J. del Campo, J.P. Esquivel, F. Giroud, S.D. Minteer, N. Sabate, *J. Power Sources* 326 (2016) 410–416.
- [50] M.J. González-Guerrero, F.J. del Campo, J.P. Esquivel, D. Leech, N. Sabaté, *Biosens. Bioelectron.* 90 (2017) 475–480.
- [51] L. del Torno-de Román, M. Navarro, G. Hughes, J.P. Esquivel, R.D. Milton, S.D. Minteer, N. Sabaté, *Electrochim. Acta* 282 (2018) 336–342.
- [52] I. Shitanda, S. Nohara, Y. Hoshi, M. Itagaki, S. Tsujimura, *J. Power Sources* 360 (2017) 516–519.
- [53] I. Shitanda, S. Kato, S. Tsujimura, Y. Hoshi, M. Itagaki, *Chem. Lett.* 46 (2017) 726–728.
- [54] I. Shitanda, M. Momiyama, N. Watanabe, T. Tanaka, S. Tsujimura, Y. Hoshi, M. Itagaki, *ChemElectroChem* 4 (2017) 2460–2463.